Available online at www.sciencedirect.com

ScienceDirect

Procedia CIRP 127 (2024) 230–235

www.elsevier.com/locate/procedia

10th CIRP Conference on Assembly Technology and Systems (CIRP CATS 2024)

High-Speed DED-LB: Analysis of Process Control Variables as Enabler for Remanufacturing of Unique Products

Helena Wexel*[a], Patrick Fischmann[a], Johannes Schubert[a], Frederik Zanger[a]

[a] *wbk Institute of Production Science, Karlsruhe Institute of Technology, Kaiserstr. 12, 76131 Karlsruhe, Germany*

* Corresponding author. Tel.: +49 1523 950 2637; fax: +49 721 608-45005. E-mail address: helena.wexel@kit.edu

Abstract

The implementation of sustainable production patterns in the sense of a circular economy is becoming increasingly important due to the rising consumption of resources. In addition, remanufacturing enables the technological sovereignty of company locations. The aim of remanufacturing is to return used products to the market in an as-new or even better condition than initial new products. To achieve this, flexible, semi-autonomous production is needed, which requires a coordinated, adaptable production system. This can be achieved by combining additive manufacturing (AM) and machining. Powder-based high-speed directed energy deposition using a laser beam (DED-LB) is particularly suitable for this application. High-speed DED-LB enables multifunctional structures and the combination of multiple metal powders in a single component. In addition, by specifically influencing the cooling rates, high-speed DED-LB is capable of producing metal parts with high hardness and high strength. Modern DED-LB systems include 5-axis features, allowing material to be applied to irregular geometries. To unlock the full potential of the DED-LB process, suitable process parameters for thick- and thin-walled components must be derived. Therefore, the relationship between process parameters, resulting geometries and process influences on microstructure must be known. This will help to overcome technical challenges such as repeatability and quality, as well as difficulties caused by cumulative defects, and create a basis for reliable reprocessing in the sense of a circular economy.

Keywords: High-Speed Directed Energy Deposition; Additive Manufacturing; Remanufacturing

1. Introduction

In nearly all industries and sectors of the economy, repair costs and production downtimes are significant. Furthermore, the implementation of sustainable production patterns is becoming increasingly important [1]. Extending the life of components through remanufacturing can significantly improve lifecycle sustainability and offer immense cost savings [2]. Studies have shown that the specific energy requirement for metal-based AM processes can be higher than for subtractive processes [3]. Additive manufacturing technologies are therefore sustainable not because of their energy efficiency, but because they enable production strategies such as circular economy. Remanufacturing allows used components to be returned to the market in as-new or even better condition than the original new products. The consistent implementation of a circular economy, in which components are remanufactured, is achieved with a process combination of additive manufacturing and the subsequent machining required for the production of functional surfaces. The goal of flexible, semi-autonomous production can be achieved here by combining a 5-axis high-speed DED-LB system with multiple material supply and a 5-axis mill-turn machining center. The combination of the two machines, with multiple sensors and an automation offers an opportunity for sustainable economic remanufacturing.

As an additive manufacturing (AM) process, powder-based high-speed directed energy deposition using a laser beam (DED-LB) offers the possibility of building near-net-shape

10.1016/j.procir.2024.07.040

components by successive addition of material. Along with powder bed fusion by a laser beam (PBF-LB), DED is considered as one of the most important processes for the additive processing of metal powders [4]. Compared to other metal-based additive manufacturing processes, DED is characterized by significantly higher build-up rates. Shifting the powder focus above the substrate allows the added powder to melt prior to deposition [2]. By eliminating the time required to melt the powder in the melt pool, processing speeds of up to 200 m/min are possible, further reducing process times for high-speed DED [5]. DED-LB enables the design of multifunctional structures and the combination of several powder materials in one component [6]. Furthermore, state-of the art systems allow material deposition on uneven geometries using a 5-axis functionality. By adjusting the cooling rates, components of high hardness and high strength can be produced [4]. To enable sustainable economic remanufacturing of components, it is essential to derive suitable process control variables considering the existing component geometry in order to ensure reliability and consistent quality of the buildup components. Database management allows process windows to be defined for different materials and geometries. In this way, technical challenges, such as reproducibility and consistent quality, as well as difficulties due to cumulative defects, can be overcome. Thereby, the basis for reliable reprocessing in the sense of a circular economy can be created.

Nomenclature

AM	additive manufacturing
DED	directed energy deposition
LB	laser beam
PBF	powder bed fusion
γ	hatch distance
E_{eff}	effective energy
$E_{V,HS\ DED\text{-}LB}$	energy volume density for High Speed DED-LB
$E_{V,PBF\text{-}LB}$	energy volume density for PBF-LB
F	powder density
h	layer height
h_{th}	theoretical layer height
$\dot{m}$	powder mass flow
ρ_{316L}	density of 316L
P_L	laser power
v	processing speed

2. State of the Art

High-speed DED-LB is a new process variant of conventional powder-based DED [4]. The powder focus is located above the substrate. As a result, the powder supplied is melted above the substrate surface and is fed to the melt pool in liquid state [2]. This eliminates the time required for the particles to melt in the melt pool on the substrate surface, which increases the possible processing speed [6].

Various process control variables have a significant influence on the process result [7]. According to Greco et al., especially the variables of laser power, powder mass flow and processing speed, and their relationship to each other, have a significant effect on the mechanical properties of the component [8]. An experimental approach to identify relevant process control variables and, in particular, their appropriate ratios is described for conventional DED of 316L by Sciammarella et al. [9]. Schmidt et al. investigated the density, microstructure and hardness of 316L cubes produced by high-speed DED-LB with a defined parameter set and achieved a maximum relative density of 99.38% [7]. In the work by Li et al., three different build-up strategies for high-speed DED-LB of AISI 4340 steel were investigated while maintaining the process control variables, leading to porosities between 0.15 % and 3.45 % [10]. Platz et al. performed density and microhardness measurements on 17-4 PH specimens produced by high-speed DED-LB and determined relative density values of up to 99.49 % using optical porosity analysis (Platz et al. 2022) [5]. In the work of Schaible et al., cubic volumes were produced by high-speed DED-LB using 316L and different deposition strategies commonly used in DED-LB were tested for their transferability [11].

Accordingly, a sufficient process window for the production of 316L samples using DED-LB has not yet been defined. Furthermore, the influence of the sample geometry on the process control variables has not been considered in previous investigations. In order to exploit the full potential of the high-speed DED-LB process, the aim of this work is to derive suitable process control variables for thick and thin-walled components and to lay the foundations for a suitable process window. For this purpose, the relationship between selected process control variables and resulting geometries on the manufactured component must be known. In the long term, this should enable an automated adjustment of the process control variables in dependency of the manufactured geometries. The relative density is a comparative value that indicates the ratio between material and pores in the generated structure [7] and is used in this work as an indicator for the generated material quality and the influence of the process parameters. The process window validated by the density measurement will serve as a basis for future reliable reprocessing in the sense of a circular economy.

3. Materials and Methods

For the present study, 316L powder from m4p material solutions GmbH with a particle size between 20 µm and 63 µm was used and deposited on substrate plates of cold-rolled 1.0038 steel. All specimens were manufactured on a pE3D high-speed DED-LB system of Ponticon GmbH. The maximum speed of the pE3D system is 200 m/min and the maximum acceleration is 50 m/s^2. The powder conveyor used was a PF2-2 MFR model from BLC Lasercladding GmbH. A high-power diode laser LDF 6000-40 from Laserline GmbH with a maximum laser power of 6 kW and a coaxial powder nozzle type RP13 from Laserline GmbH were used.

In this study, the process control variables laser power, powder mass flow and processing speed were varied fully factorially and optically investigated using the scanCONTROL 3000-50 from MICRO EPSILON. For each parameter set, 10 mm long single-tracks and 10 tracks for cuboids with an edge length of 10 mm were built, each with 10 layers height.

All samples were produced with a hatch distance of 0.5 mm, a laser spot diameter of 1 mm and a nozzle-substrate stand-off distance of 14 mm. The scanning strategy was bidirectional. The shielding gas flow rate was 14 l/min and the carrier gas flow rate was 6 l/min. Further parameters are listed in Table 1.

Table 1. Process control variables parameter study.

Process control variables	Laser power in W	Powder mass flow rate in g/min	Processing speed in m/min
Considered range	1000 – 2600	12 – 36	35– 80
Step size	200	8	15

For PBF-LB, the volume energy density $E_{V,PBF\text{-}LB}$ has proven to be useful for assessing the energy input. $E_{V,PBF\text{-}LB}$ in J/mm³ is defined as laser energy per volume and can be calculated according to Eq. (1) with laser power P_L, hatch distance γ, layer height h and processing speed v [12]:

$$E_{V,PBF-LB} = \frac{P_L}{\gamma * h * v} \quad (1)$$

In order to correlate the selected parameter sets, it is also necessary to define a comparable value for high-speed DED-LB to represent the applied energy. The parameters effective energy E_{eff} and powder density F are often used to evaluate the classical DED method [13 - 15]. The effective energy E_{eff} in J/mm² is defined in Eq. (2) [16]:

$$E_{eff} = \frac{P_L}{\gamma * v} \quad (2)$$

The powder density F in g/mm² is given in Eq. (3) with the powder mass flow ṁ [16]:

$$F = \frac{\dot{m}}{\gamma * v} \quad (3)$$

The theoretical layer height h_{th} in mm can be defined according Eq. (4) with an ideal density of 316L ρ_{316L} = 7.99 g/cm³:

$$h_{th} = \frac{F}{\rho_{316L}} = \frac{\dot{m}}{\rho_{316L} * \gamma * v} \quad (4)$$

If the layer height in (1) is replaced by the theoretical layer height (4), the relationship for the volume energy density $E_{V,HS\text{-}DED}$ in J/mm³ given in Eq. (5) is obtained:

$$E_{V,HS\ DED-LB} = \frac{P_L * \rho_{316L}}{\dot{m}} \quad (5)$$

Koß et al. emphasize that in high-speed DED-LB most of the laser radiation is absorbed by the powder particles and also define the energy volume density for the process according to Eq. (5) [17]. Therefore, $E_{V,HS\ DED\text{-}LB}$ given in Eq. (5) is used to evaluate the experimental results of this work. From the full factorial parameter study, the expected build height for each parameter set used was evaluated using a MICRO EPSILON laser line scanner. From the optical evaluation, the best three parameter sets were selected to build the cubes with an edge length of 10 mm. The parameter sets were selected regarding a comparatively good surface result without any visible pores or ripples. In addition, a wide range of processing speeds was considered. To investigate the influence of the laser power, parameter sets C1 to C3 were reduced (C_A) or increased (C_B) by 100 W each, respectively. At 2,400 W, significant spattering and rapid nozzle contamination were observed, therefore the C3_B variation was omitted. The selected parameter sets for the cube shaped samples and the volume energy densities defined according to (5) are shown in Table 2.

Table 2. Process control variables cuboids.

Sample		Laser power in W	Powder mass flow rate in g/min	Processing speed in m/min	Volume energy density in J/mm³
C1		1,200	12	35	47.8
	A	1,100			43.8
	B	1,300			51.8
C2		2,000	28	50	34.1
	A	1,900			32.4
	B	2,100			35.8
C3		2,400	36	80	31.9
	A	2,300			30.5

Parameter sets C1 to C3 were used to define the process control variables for single-tracks. The laser power for the parameter sets S1 to S3 has been adjusted downwards for variants D, E and F due to the reduced heat dissipation. The single-track process control variables and volume energy densities are listed in Table 3.

Table 3. Process control variables single-tracks.

Sample		Laser power in W	Powder mass flow rate in g/min	Processing speed in m/min	Volume energy density in J/mm³
S1	C	1200	12	35	47.8
	D	700			27.9
	E	600			23.9
	F	500			19.9
S2	C	2000	28	50	34.1
	D	1500			25.6
	E	1400			23.9
	F	1300			22.2
S3	C	2400	36	80	31.9
	D	1500			19.9
	E	1400			18.6
	F	1300			17.3

Density measurement methods play an important role in assessing the quality of DED deposition [18]. Several methods have been established to determine the density of additively manufactured samples. For comparison, density measurements were performed both by using the Archimedean principle in distilled water and an optical porosity analysis of the cube-shaped samples. Images were taken perpendicular to the build direction using a Keyence VHX-970 F digital microscope at

100x magnification. To represent the entire surface, three images per sample were taken and the mean and standard deviation of the relative density were calculated.

4. Results

The means and standard deviations of the Archimedean density measurements and the optical analysis for the cubic samples are shown in Fig. 1. The results show that the Archimedean density is always lower than the density values obtained from optical porosity analysis of micrographs. However, the relationship between the densities within each method is comparable. The lower laser power in variant 'A' results in a decrease in relative density for each combination. For parameter set C1_B, the further increase in laser power again led to a slight decrease in relative density, while for parameter set C2_B the highest relative density of 99.91% was achieved.

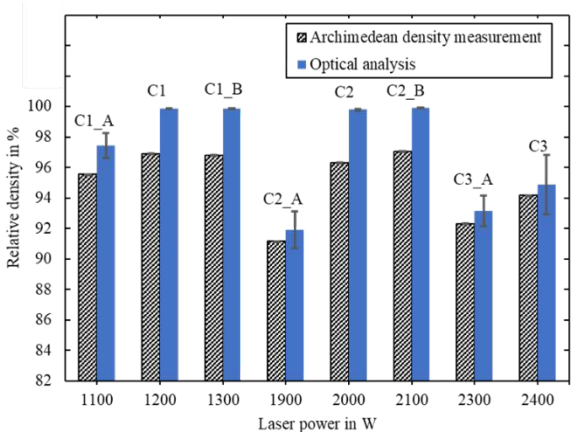

Fig. 1. Comparison of relative densities determined by Archimedean measurement and optical porosity analysis for cubic samples.

The relative density of the single-track samples was again analysed using the Archimedean principle. The means and standard deviations are shown in Fig. 2. The relative densities are lower than for cubic samples. The highest relative density of 91.26 % was obtained with parameter set S2_F.

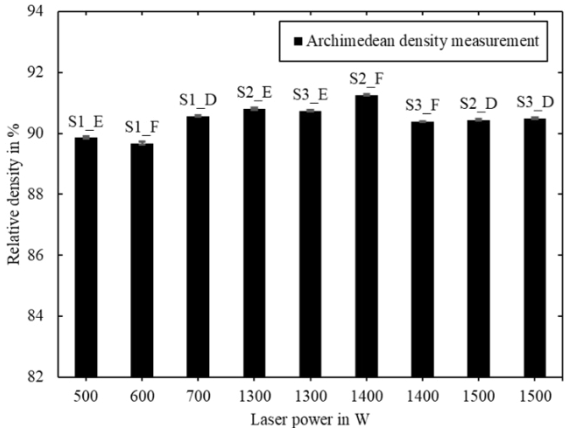

Fig. 2. Comparison of relative densities determined by Archimedean measurement for single-track samples.

In order to evaluate the influence of the introduced volume energy density according to formula (5), Fig. 3 shows the relative density determined by the Archimedean principle in dependency of the volume energy density. For a volume energy density of less than 34 J/mm^3, an increased porosity of the cubic samples can be observed. As mentioned earlier, the energy input was reduced due to the lower heat dissipation of the single-track samples. The relative density values of the single-track samples produced using the cube parameters are below 87 %. Accordingly, for the single-track samples, an excessively large laser power and thus, a too high volume energy density leads to a significant increase in porosity.

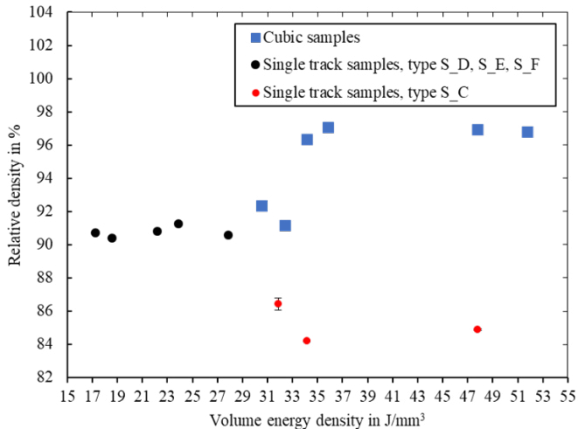

Fig. 3. Influence of volume energy density on relative density, determined by Archimedean measurement for single-track samples.

Fig. 4 shows exemplary micrographs for the cubic samples. For samples C1_A, C2_A, C3 and C3_A, the majority of the pores are large lack-of-fusion pores. In addition, the overall view of the sample cross section shows that the pores of samples C2_A, C3 and C3_A were formed between the individual scan tracks. The micrographs of samples C1, C1_B and C2_B show cracks in addition to smaller keyhole like pores. During the process, the material undergoes rapid heating and cooling rates, leading to high solidification shrinkage stresses in the deposited layer and thus, to cracking [19].

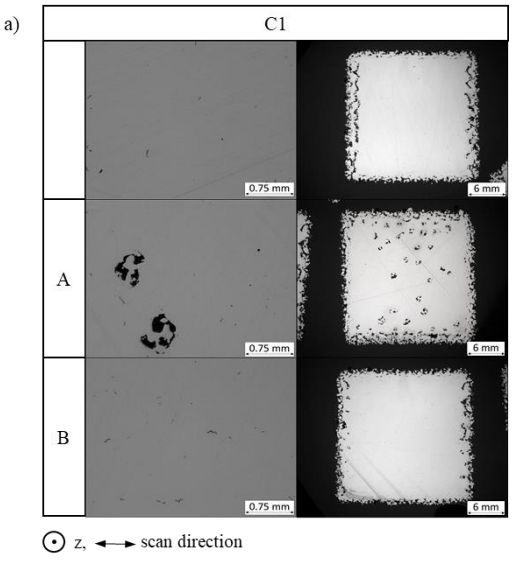

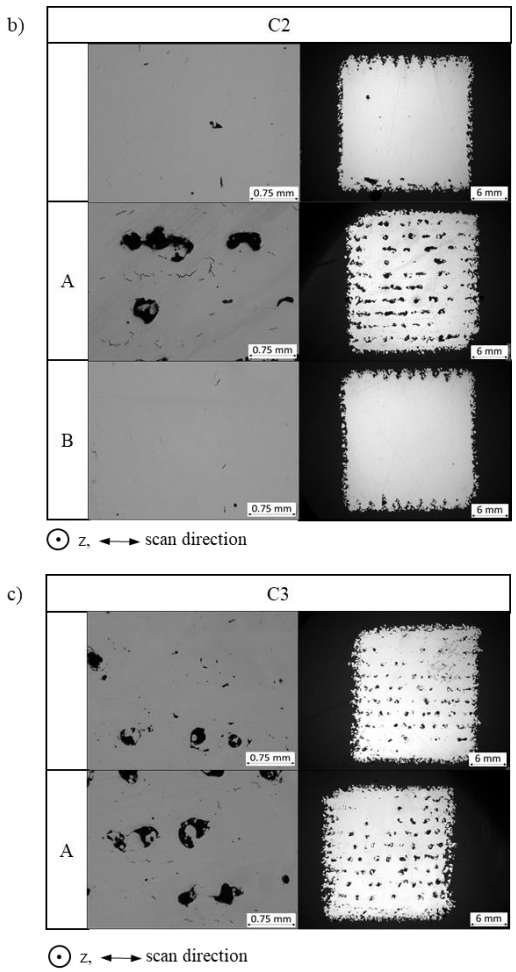

Fig. 4. Exemplary microscopic images of cubic samples, a) samples C1, C1_A, C1_B, b) samples C2, C2_A, C2_B, c) samples C3, C3_A

Exemplary microscopic images of the single-track samples are shown in Fig. 5. They show that the material density varies along the component height. For samples S2_D, S2_E and S2_F, there is a gradual transition of denser material from the lower layers in S2_D to the upper layers in S2_F with decreasing laser power. The density achievable for a given laser power therefore varies as a function of component height.

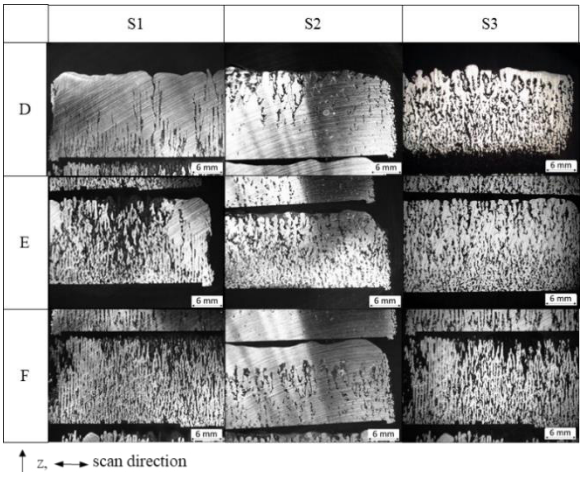

Fig. 5. Exemplary microscopic images of cubic samples.

5. Discussion

This study provides a first introduction to a wide field of new possibilities for the derivation of optimized process control variables opened up by the use of high-speed DED-LB for AM. Accordingly, the initial data points serve as starting point for future investigations. When evaluating the results of the density measurements, the chosen method must be considered. The relationship between the density values within each method was found to be comparable. However, the Archimedean density values are lower than those obtained by optical porosity analysis. Therefore, the density values of a series of measurements can be compared regardless of the measurement method used. When comparing with values obtained by other methods, the discrepancy must be considered. It should be noted that Archimedean density measurement takes the entire sample into account when determining density, whereas optical porosity analysis uses only a limited area of the interior of the component for evaluation. As a result, the results of optical porosity analysis are subject to greater variation. With the Archimedean method, it should be noted that the high surface roughness of the as-built samples favors the adhesion of small air bubbles. This can influence the measurement result towards a lower density value [18]. This effect is more pronounced in the lighter single-track samples.

In total, a density > 99.7 % could be achieved for volumetric samples with four different parameter sets. A reduction in laser power resulted in a decrease in component density for the cubic samples due to the increased number of lack-of-fusion pores. These pores are caused by binding defects and are the result of too little energy input during the process [20]. The literature documents an increased occurrence of these lack-of-fusion pores in areas where two exposure regions are adjacent [21]. The pores of samples C1_A, C2_A, C3 and C3_A can be located between the individual scan tracks. With increasing energy input the porosity could be reduced. For the samples C1, C2 and C2_B, keyhole like pores can be seen in the microscopy images. These pores form as a result of excessive energy input. In addition, cracks can be seen in these samples, especially in sample C1_B. During the high-speed DED-LB process, the material experiences very high heating and cooling rates, leading to high solidification shrinkage stresses in the deposited layer and thus, to cracking. Especially austenitic stainless steels are more susceptible to solidification cracking than low carbon steels [19].

Thus, both too low and too high laser power lead to different defects, which have a negative effect on the properties of the component. Already a change in laser power of 100 W has significant effects on the built-up geometry. As a result, it is necessary to define a suitable process window for manufacturing high density components. The volume energy density introduced according to (5) can be used to evaluate the process window. For cubic samples, a decrease of the density values for $E_{V,\,HS\text{-}DED} \leq 34$ J/mm^3 could be observed. When evaluating the process window, the component geometry must be considered. Thin-walled geometries, such as the single-track samples, with lower heat dissipation achieve significantly

lower density values than larger component volumes for the same volume energy density.

When evaluating the microscopic images of the single-track samples, it should be noted that it cannot be assumed that the sections represent the center of the samples. Consequently, a statement about the density of the single-track samples can only be made using the Archimedean density measurement. However, with constant laser power over the component height, a variable porosity profile over the component height could be determined for the single-track samples. Accordingly, for thin-walled geometries, the change in heat dissipation as a function of component height must be considered and therefore, the laser power must be reduced as the component height increases.

6. Conclusion

In this work, several process control variables have been investigated and initial data were generated to determine a suitable process window for high-speed DED-LB. When evaluating the influence of the process control variables, the geometry of the component must be considered. Furthermore, the resulting porosity differs depending on the measurement method chosen, but within a method, the results can be related to each other. If the geometry results in a change in heat dissipation, e.g. for thin-walled components, the process control variables must be adjusted accordingly. The exact strategy for the design of thin-wall components will be the subject of further investigation. For example, for single-track components, the laser power could be reduced as the component height increases. In addition, further data points will need to be collected to generate an accurate process window for manufacturing high-density components. With the results of this study, the foundation for a flexible, semi-autonomous production is laid to enable the reliable remanufacturing of components with variable geometry in the future.

References

[1] Mankelow, J., Nyakinye, M., & Petavratzi, E. (2021). Ensure sustainable consumption and production patterns. *Geosciences and the Sustainable Development Goals*, 283-311.

[2] Schopphoven, T. (2020). *Experimentelle und modelltheoretische Untersuchungen zum Extremen Hochgeschwindigkeits-Laserauftragschweißen* (Doctoral dissertation, Dissertation, RWTH Aachen University, 2019).

[3] Ehmsen, S., Glatt, M., & Aurich, J. C. (2023). Influence of process parameters on the power consumption of high-speed laser directed energy deposition. *Procedia CIRP*, *116*, 89-94.

[4] Tang, Z. J., Liu, W. W., Wang, Y. W., Saleheen, K. M., Liu, Z. C., Peng, S. T., ... & Zhang, H. C. (2020). A review on in situ monitoring technology for directed energy deposition of metals. *The International Journal of Advanced Manufacturing Technology*, *108*, 3437-3463.

[5] Platz, J., Schmidt, M., Gutzeit, K., Kirsch, B., & Aurich, J. C. (2022). Additive Fertigung von 17-4 PH Edelstahl durch Hochgeschwindigkeits-Laserauftragschweißen. *Zeitschrift für wirtschaftlichen Fabrikbetrieb*, *117*(7-8), 456-460.

[6] Schaible, J., Sayk, L., Schopphoven, T., Schleifenbaum, J. H., & Häfner, C. (2021). Development of a high-speed laser material deposition process for additive manufacturing. *Journal of Laser Applications*, *33*(1).

[7] Schmidt, M., Greco, S., Kirsch, B., & Aurich, J. C. (2022). Analysis of Material Properties of Additively Manufactured Workpieces Using High-Speed Laser DirectedEnergy Deposition. In *Production at the Leading Edge of Technology: Proceedings of the 11th Congress of the German Academic Association for Production Technology (WGP), Dresden, September 2021* (pp. 357-365). Springer International Publishing.

[8] Greco S., Schmidt M., Kirsch B., Aurich J.C. (2021). Center for applied additive manufacturing-influence of process parameters during high-speed laser direct energy deposition. *WT Werkstattstechnik*, 111 (6), pp. 368 - 371

[9] Sciammarella, F. M., & Salehi Najafabadi, B. (2018). Processing parameter DOE for 316L using directed energy deposition. *Journal of Manufacturing and Materials Processing*, *2*(3), 61.

[10] Li, T., Zhang, L., Bultel, G. G. P., Schopphoven, T., Gasser, A., Schleifenbaum, J. H., & Poprawe, R. (2019). Extreme high-speed laser material deposition (EHLA) of AISI 4340 steel. *Coatings*, *9*(12), 778.

[11] Schaible, J., Hausch, D., Schopphoven, T., & Häfner, C. (2022). Deposition strategies for generating cuboid volumes using extreme high-speed directed energy deposition. *Journal of Laser Applications*, 34(4).

[12] Wei, K., Gao, M., Wang, Z., & Zeng, X. (2014). Effect of energy input on formability, microstructure and mechanical properties of selective laser melted AZ91D magnesium alloy. *Materials Science and Engineering: A*, *611*, 212-222.

[13] Shim, D. S., Baek, G. Y., Seo, J. S., Shin, G. Y., Kim, K. P., & Lee, K. Y. (2016). Effect of layer thickness setting on deposition characteristics in direct energy deposition (DED) process. *Optics & Laser Technology*, *86*, 69-78.

[14] Lin, P. Y., Shen, F. C., Wu, K. T., Hwang, S. J., & Lee, H. H. (2020). Process optimization for directed energy deposition of SS316L components. *The International Journal of Advanced Manufacturing Technology*, *111*, 1387-1400.

[15] Aleksandr, K., Ferdinando, S., Joel, R., Joel, C., Jordan, M., & Thomas, J. (2021). Effect of direct energy deposition parameters on morphology, residual stresses, density, and microstructure of 1.2709 maraging steel. *The International Journal of Advanced Manufacturing Technology*, *117*(3-4), 1287-1301.

[16] Toyserkani, E., Khajepour, A., & Corbin, S. F. (2004). *Laser cladding*. CRC press.

[17] Koß, S., Ewald, S., Bold, M. N., Koch, J. H., Voshage, M., Ziegler, S., & Schleifenbaum, J. H. (2021). Comparison of the EHLA and LPBF process in context of new alloy design methods for LPBF. *Advanced Materials Research*, *1161*, 13-25.

[18] Spierings, A. B., Schneider, M. U., & Eggenberger, R. J. R. P. J. (2011). Comparison of density measurement techniques for additive manufactured metallic parts. *Rapid Prototyping Journal*, *17*(5), 380-386.

[19] Yu, J., Rombouts, M., & Maes, G. (2013). Cracking behavior and mechanical properties of austenitic stainless steel parts produced by laser metal deposition. *Materials & Design*, 45, 228-235.

[20] Tang, M. (2017). *Inclusions, porosity, and fatigue of AlSi10Mg parts produced by selective laser melting* (Doctoral dissertation, Carnegie Mellon University).

[21] Richard, H. A., Schramm, B., & Zipsner, T. (Eds.). (2017). *Additive Fertigung von Bauteilen und Strukturen*. Springer-Verlag.